Design and analysis of a hybrid-excited coaxial magnetic gear utilising DC field excitation coils

Article *in* PRZEGLĄD ELEKTROTECHNICZNY · September 2025

DOI: 10.15199/48.2025.09.26

4 authors, including:

Sarweash Rao Tharma Raja
Technical University of Malaysia Malacca
3 PUBLICATIONS **0** CITATIONS
SEE PROFILE

Mohd Firdaus bin Mohd Ab Halim
Technical University of Malaysia Malacca
40 PUBLICATIONS **137** CITATIONS
SEE PROFILE

Fauzi Ahmad
Technical University of Malaysia Malacca
38 PUBLICATIONS **369** CITATIONS
SEE PROFILE

OPEN ACCESS

PRZEGLĄD ELEKTROTECHNICZNY

Sarweash Rao Tharma RAJA[1], Mohd Firdaus Mohd Ab HALIM[2], Fauzi AHMAD[3], Syed Muhammad Naufal Syed OTHMAN[4]

ORCID: [1]0009-0004-4633-6340, [2]0000-0001-6965-9143, [3]0000-0002-0790-7348, [4]0000-0002-3104-7480

DOI: 10.15199/48.2025.09.26

Design and analysis of a hybrid-excited coaxial magnetic gear utilising DC field excitation coils

Projekt i analiza hybrydowo-wzbudnego współosiowego koła magnetycznego wykorzystującego cewki wzbudzające pole prądu stałego

[1] Sarweash Rao Tharma Raja, Graduate Research Assistant, Master of Science (MSc) in Electrical Engineering, Faculty of Electrical Technology and Engineering, Universiti Teknikal Malaysia Melaka, Melaka, Malaysia, e-mail: m112410008@student.utem.edu.my

[2] Ts. Dr. Mohd Firdaus bin Mohd Ab Halim, Faculty of Electrical Technology and Engineering, Universiti Teknikal Malaysia Melaka, Melaka, Malaysia, e-mail: mohd.firdaus@utem.edu.my

[3] Ir. Ts. Dr. Fauzi bin Ahmad, Faculty of Mechanical Technology and Engineering, Universiti Teknikal Malaysia Melaka, Melaka, Malaysia, e-mail: fauzi.ahmad@utem.edu.my

[4] Syed Muhammad Naufal Syed Othman, Graduate Research Assistant, Doctorate of Philosophy (PhD) in Electrical Engineering, Research Center for Applied Electromagnetics, Universiti Tun Hussein Onn Malaysia, Johor, Malaysia, e-mail: he160080@student.uthm.edu.my

Correspondence address: mohd.firdaus@utem.edu.my

Abstract: This paper presents a hybrid-excited coaxial magnetic gear (HE-CMG) with direct current (DC) field excitation coils (FECs). In the outer rotor, the north permanent magnets (PMs) are replaced with cylindrical iron poles, slotted to form a stator slot-like structure with defined teeth, and DC FECs are wound around the teeth. A 2D finite element analysis (FEA) shows that although torque is reduced compared to conventional CMGs, the design lowers PM usage and has the potential to match or exceed traditional torque transmission in future developments.

Keywords: consequent pole, magnetic gear, hybrid excitation, rare earth permanent magnet

Streszczenie: W niniejszym artykule przedstawiono hybrydowo-wzbudzoną współosiową przekładnię magnetyczną (HE-CMG) z cewkami wzbudzenia pola prądu stałego (FEC). W wirniku zewnętrznym północne magnesy trwałe (PM) zostały zastąpione cylindrycznymi, żelaznymi biegunami, rowkowanymi w celu utworzenia struktury przypominającej żłobek stojana z określonymi zębami, a cewki wzbudzenia pola prądu stałego (FEC) są nawinięte wokół zębów. Dwuwymiarowa analiza elementów skończonych (MES) pokazuje, że pomimo mniejszego momentu obrotowego w porównaniu z konwencjonalnymi przekładniami CMG, konstrukcja ta zmniejsza zużycie magnesów trwałych i ma potencjał, aby dorównać lub przewyższyć tradycyjne przenoszenie momentu obrotowego w przyszłych rozwiązaniach.

Słowa kluczowe: biegun następczy, przekładnia magnetyczna, wzbudzenie hybrydowe, magnes trwały z metali ziem rzadkich

Introduction

As electrification accelerates across transportation, robotics, and renewable energy systems, the need for efficient, compact, and low-maintenance torque transmission solutions becomes increasingly critical. Magnetic gears (MGs) have emerged as a promising alternative to conventional mechanical gear systems, offering contactless torque transmission with reduced noise, zero lubrication requirements, and intrinsic overload protection [1]. Among various MG topologies, coaxial magnetic gears (CMGs) are particularly notable for their symmetrical design and high torque density, wherein all the permanent magnets (PMs) actively contribute to torque generation [2]. However, CMGs heavily depend on rare earth permanent magnets (REPMs), which, despite their superior magnetic properties, present significant challenges in terms of cost, sustainability, and supply chain risks [3].

A review of flux excitation methods in CMGs reveals three primary classifications, based on the flux excitation sources employed in the inner and outer pole pair rotors, as illustrated in Figure 1. The first category comprises conventional CMG, which rely exclusively on REPM materials, such as NdFeB, in inner and outer rotors [4-6]. The second category is electromagnetic CMG, which replaces PMs with field windings in both rotors [7,8]. The third category, hybrid-excited CMGs, integrates the benefits of both PM and field winding

excitation [9,10]. In this configuration, the inner rotor utilizes REPMs, while the outer rotor incorporates REPMs and field excitation windings. However, despite these developments, the current body of designs remains limited in quantity and diversity. Therefore, pursuing new iterations of CMG configuration that focus on reducing PM volume, while offering a practical torque transmission system, presents a promising research direction. The exploration of such innovative designs is essential to minimize environmental impact and advance sustainable technologies for future generations [11].

In this paper, a hybrid-excited consequent pole (CP) coaxial magnetic gear (HE-CMG) featuring direct current (DC) field excitation coils (FECs) wound within the stator's enclosed slots is proposed. By combining excitation from both PMs and FECs, the proposed design effectively reduces the reliance on REPM, offering practical torque transmission capabilities and a cost-effective solution for sustainable applications.

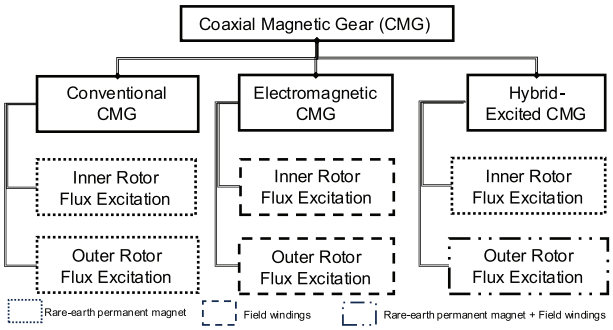

Fig. 1. Classification of CMG based on flux excitation method

Principle of Operation of CMG and RPMG

Figure 2 illustrates the fundamental structure of a CMG, which consists of three main elements: an inner rotor featuring inner pole pairs (IPPs), an outer rotor with outer pole pairs (OPPs), and a magnetic flux modulator ring (also known as the ferromagnetic pole piece (FMP) ring or FMP rotor) positioned between the IPP rotor and OPP rotors. The core operating principle of CMGs relies on air-gap flux modulation, where the interaction between permanent magnet (PM) rotors and the stationary FMP rotor generates space harmonics essential for effective torque transmission. The condition required for optimal torque transmission capability is expressed as:

$$n_S = p_i + p_o \tag{1}$$

where n_S denotes the number of FMPs, p_i and p_o represent the inner and outer PM pole pairs, respectively. CMGs allow independent rotation of all three components, enabling various configurations depending on which element is stationary. This results in three possible gear ratios, $G_{R1, R2, R3}$ for torque multiplication applications:

$$G_{R1} = \frac{p_o}{p_i}, G_{R2} = \frac{n_s}{p_i}, G_{R3} = \frac{n_s}{p_o} \tag{2}$$

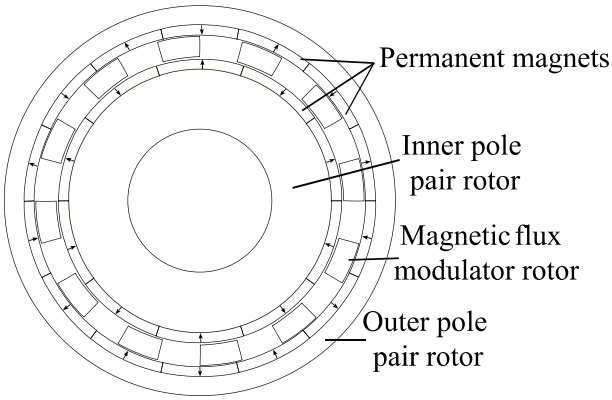

Fig. 2. Conventional CMG

To maximize transmission ratio and the associated output torque, this study designates the IPP rotor as the input rotor, and the FMP rotor as the output rotor, while keeping the OPP rotor stationary. This configuration is known as the rotating pole piece coaxial magnetic gear (RPMG) [12]. According to equation (2), this arrangement achieves a higher gear ratio than the traditional CMG configuration with an equivalent number of pole pairs.

Design and Configuration of CP-RPMG and HE-CMG

Several key modifications are introduced to develop a hybrid excited coaxial magnetic gear (HE-CMG) that reduces the volume of PMs while maintaining practical torque multiplication capabilities. First, the number of PMs in the OPP rotor of the RPMG is halved by removing all radially magnetized, outward-facing north-pole PMs. These removed PMs are then replaced with cylindrical (non-salient) iron poles, forming a consequent pole (CP) structure in the OPP rotor. This design is called the consequent pole rotating pole piece magnetic gear (CP-RPMG), as shown in Figure 3. This modification initially reduces the effective number of OPPs, leading to a lower total PM volume. However, it also results in reduced torque transmission capability. For instance, a conventional RPMG configures 5 IPPs, 7 OPPs, and 12 FMPs. By removing 3.5 of north-facing OPPs, the number of OPPs reduces to 3.5, leaving only 8.5 FMPs and violating

equation (1), thereby preventing maximum torque transmission.

Nevertheless, in CP-RPMG, the remaining PMs with identical magnetization directions are placed alternately with the cylindrical iron poles. These iron poles act as substitute magnetic poles, where adjacent PMs induce magnetic flux in the iron poles, effectively generating induced north poles. However, the resulting magnetic field strength is comparatively weaker since these are not actual PMs. The CP-RPMG is further developed into a hybrid-excited configuration by integrating field excitation coils (FECs) into the cylindrical iron poles to enhance the magnetic field of these induced north poles. Hybrid-excited electrical machines inspire this concept. In this hybrid excitation magnetic gear configuration, PMs and electromagnets are used to establish magnetic fields in the air gaps, thus combining the advantages of permanent magnet and electromagnetic gears [9,10,13].

Figure 4 presents the proposed HE-CMG topology. In this design, the cylindrical iron poles from the CP-RPMG are slotted to form closed stator-like slots with defined teeth between them. These teeth serve as the core for the FECs, which are wound concentrically to create electromagnets. The teeth are made of steel sheet, the same material as the yoke, to conduct magnetic flux effectively, and the electromagnets are energized using a direct current (DC) source to establish stronger north poles via current-induced magnetization.

In other words, to address the torque reduction due to the removal of 3.5 PM poles, the hybrid excitation method reintroduces an equivalent number of electromagnetic poles using FECs, thereby restoring the 7 OPPs and fulfilling the required 12 FMPs in the HE-CMG. Using electromagnetic poles formed by FECs around the iron poles aims to intensify the formation of stronger north poles, thereby enhancing the magnetic interaction and improving torque

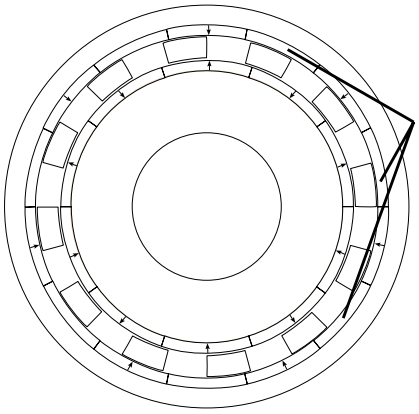

Fig. 3. CP-RPMG

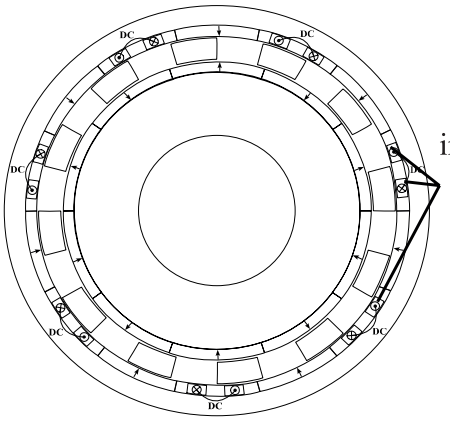

Fig. 4. Proposed HE-CMG

transmission. However, the extent to which this hybrid excitation improves performance in this current configuration remains a key focus of investigation in this research. The conventional N-S-N-S PM arrangement in the IPP rotor is retained. Meanwhile, the excitation pattern in the OPP rotor (stator) is defined as S-O-X-S-O-X-S, where S represents south-pole PMs, O denotes current exiting the page, and X represents current entering the page.

Each stator tooth is wound using a concentrated winding, meaning a single coil is wrapped around one tooth (O-X), thus forming a compact electromagnet to replace the removed PMs. Since the coil span equals one slot pitch and does not overlap adjacent teeth, this configuration is referred to as a non-overlapping or tooth-coil winding [14]. Concentrated winding can reduce copper losses in permanent magnet machines [15]; however, this method introduces more spatial harmonics than distributed windings [16]. With concentrated winding, the winding resistance is decreased, reducing copper losses, as the coil ends can be manufactured shorter than those of distributed windings [17]. Moreover, it supports modular design, ease of manufacturing, and improved maintenance access [18].

Methodology

Finite element analysis (FEA) is performed using JMAG Designer to evaluate the electromagnetic performance of the RPMG and proposed HE-CMG topology. All simulations are conducted in two-dimensional (2D) transient mode. The performance of the proposed HE-CMG is compared against that of the RPMG. Both models are designed with identical geometric and material properties to ensure a fair and meaningful comparison, as outlined in Table 1. In both configurations, the IPP rotor is mechanically coupled to the prime mover, functioning as the

input, the FMP rotor acts as the output connected to the load, and the OPP rotor remains stationary. Surface-mounted arc-shaped PMs with radial magnetisation are employed in inner and outer rotor assemblies. The rotational speed condition of the IPP rotor is set at 120 rpm, while the FMP rotor operates at 50 rpm, rotates in the same direction, corresponding to a transmission ratio of 2.4. The study investigates the torque transmission characteristic by evaluating dynamic torque performance through simulations over one complete mechanical rotation and static torque performance over one full electrical cycle.

Table 1. Key design parameter of HE-CMG

Magnetic Gear Parameters	RPMG	HE-CMG
Shaft radius	34 mm	
Inner yoke radial length	29.5 mm	
Inner yoke outer radius	63.5 mm	
Inner PM radial length	5 mm	
IPP rotor outer radius	68.5 mm	
Inner air gap radial length	1 mm	
FMP radial length	10 mm	
Outer air gap radial length	0.5 mm	
Outer PM radial length	5 mm	
OPP rotor inner radius	85 mm	
Outer yoke radial length	10 mm	
Overall MG radius	95 mm	
Axial length	30 mm	
Number of IPP	5	
Number of OPP	7	
Number of FMP	12	
Gear ratio	2.4	
Speed of the IPP rotor	120 r/min	
Speed of the FMP rotor	50 r/min	
Inner yoke material	NIPPON STEEL 35H270	
Outer yoke material		
FMP material		
Grade of PM	JSOL NdFeB (Reversible)	
Remanence of PM	1.2 T	
FECs material	-	Copper
FEC's current density		0,5,10,15,20,25,30 A/mm^2
Area per cylindrical iron pole before slotted		185.13 mm^2
Area per cylindrical iron pole after slotted		118.48 mm^2
Stator slot area		33.32 mm^2 per slot
Fill factor		0.50~0.80
Area for FECs per stator slot after accounting for fill factor		16.66 mm^2~26.66 mm^2
Number of FEC turns		1

Besides that, in the HE-CMG configuration, FECs are energised using direct current (DC) sources with varying current densities up to 30 A/mm^2. Magnetic losses due to eddy currents in all components are considered in the analysis except air gaps. The thermal effects are excluded in this study, since heat generation in winding is strongly related to the current density [19]. As mentioned, the HE-CMG stator adopts a concentrated winding layout, with each FEC occupying a single stator tooth, resulting in a coil span of one slot pitch. This approach minimises the winding head length and simplifies manufacturing.

The split-open stator view of RPMG, CP-RPMG, and the proposed HE-CMG, and the corresponding equivalent electrical circuit modelled in JMAG for each FEC for HE-CMG are illustrated in Figures 5 and 6, respectively. A DC source is selected for excitation due to its ability to provide a stable and continuous magnetic field. The FEC excitation in rotor

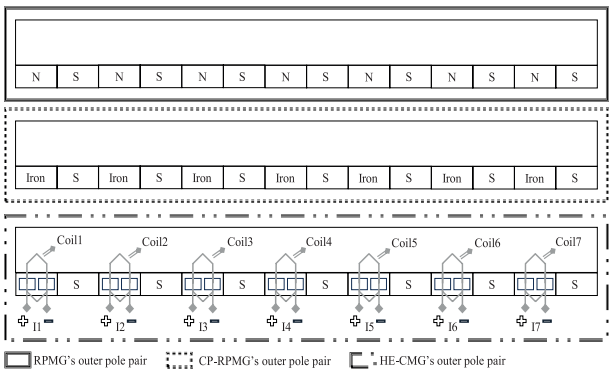

Fig. 5. The split-open stator view of RPMG, CP-RPMG, and HE-CMG

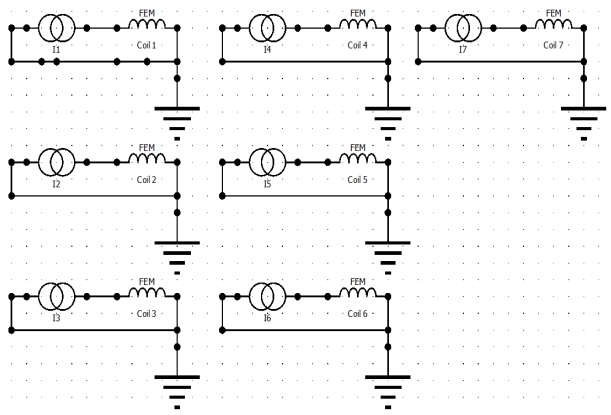

Fig. 6. Circuit representation of each concentrated winding coil in JMAG

demands brushes and slip rings to supply DC excitation, because of that, the hybrid excited machines with FEC excitation in stator are more attractive [20], eliminating the need for rotating electrical contacts. This choice enhances system reliability and simplifies practical implementation.

Estimation of Current Density for Field Excitation Coils (FECs)

To determine the required number of FEC turns, the current density, J_D is defined as the current per unit cross-sectional area of the conductor:

(3) $$J_D = \frac{I}{A}$$

where I is the total current flowing through the conductor and A is the cross-sectional area of the conductor carrying the current. In electrical machines, however, the conductors are distributed within the slots. Therefore, slot-specific parameters, including the slot area, A_{slot}, number of turns, N_{turns}, and the slot filling factor, k_{fill} must be considered.

The total current flowing through the excitation windings slot, $I_{slot,DC}$, depends on the number of turns per slot, N_{turns} and the DC excitation current, $I_{a,DC}$ supplied to each turn:

(4) $$I_{slot,\,DC} = N_{turns} I_{a,\,DC}$$

Since not all of the slot area is occupied by the conductor due to insulation and mechanical constraints, the effective copper area, A_{copper} is defined as:

(5) $$A_{copper} = k_{fill} A_{slot}$$

By substituting (4) and (5) into equation (3), the current density of the FECs becomes:

(6) $$J_{D,\,DC} = \frac{I_{slot,DC}}{A_{copper}} = \frac{N_{turns} I_{a,DC}}{k_{fill} A_{slot}}$$

A key design consideration in this study is the excitation coil configuration for the FECs. Unlike standard electrical wiring, motor windings can sustain significantly higher current densities due to better thermal management and compact slot design. In this topology, each stator slot has an area of 33.32 mm^2. With a fill factor between 0.50 and 0.80, the effective copper area per slot ranges from 16.66 mm^2 to 26.66 mm^2. To achieve a current density of 30 A/mm^2, the corresponding excitation current per slot is approximately 500 A, which excites 500 Ampere-Turns (A-t) per coil when using a single turn. However, in practical implementation, using a single large conductor may not be feasible due to the limited axial length of the machine, which restricts the ability to bend thick conductors. In such cases, the same ampere-turns can be achieved using a smaller wire with more turns, enabling flexibility in coil placement. To investigate the theoretical performance limits of the HE-CMG, the simulation considers current densities ranging from 0 A/mm^2 to 30 A/mm^2, based on achievable motor winding practices.

Parametric Torque Analysis with DC FECs

To investigate the influence of stator DC FECs on torque performance, a parametric analysis was conducted by varying the excitation current density from 0 to 30 A/mm^2. This evaluation aims to determine whether the hybrid excitation configuration in the proposed HE-CMG enhances the average torque output in response to increased excitation levels. Figures 7 and 8 present the average output and input torque simulation results under different excitation current densities. The findings indicate a consistent output and input torque increase as the excitation current density rises. Specifically, without excitation current (0 A/mm^2), the average output and input torque are 59.19 Nm and 26.34 Nm, respectively. At the maximum excitation level of 30 A/mm^2, the average output and input torque increase to 67.09 Nm and 29.57 Nm, respectively. These results demonstrate the effectiveness of the hybrid excitation system. Applying a 30 A/mm^2 excitation current yields a 13.35 % improvement in output torque and a 12.26 % increase in input torque compared to the baseline (0 A/mm^2). This validates the contribution of the stator DC FECs in enhancing the magnetic gear's torque transmission capability.

Electromagnetic Torque Characteristics

The measurement of electromagnetic torque in CMG is fundamental for evaluating performance metrics, optimizing design, assessing load capacity, analyzing efficiency, understanding dynamic behavior, performing comparative studies, and ensuring long-term reliability. Accurate torque estimation is critical to ensure the MG operates effectively under its intended application conditions.

The electromagnetic torque on both input and output rotors can be evaluated using the Maxwell stress tensor method, which is widely recognized for its

accuracy in finite element-based torque evaluation. The electromagnetic torque, T_{EM} is given by:

$$T_{EM} = \frac{L_{ef}}{\mu_0}\int_0^{2\pi} R_e^2 B_r B_\theta d\theta \tag{7}$$

where L_{ef} is the axial length of the CMG, μ_0 is the vacuum permeability, R_e is the effective radius within the air gap, B_r and B_θ are the radial and tangential components of the magnetic flux density, respectively [21].

Figure 9 illustrates the steady-state torque versus angle characteristics, showing the torque variations experienced by both the input and output rotors. The results reveal that the proposed HE-CMG generates a torque waveform similar to an RPMG. The average output torque for the RPMG and HE-CMG is 97.03 Nm and 67.09 Nm, respectively, while the average input torque is 41.85 Nm and 29.57 Nm. These values indicate a reduction of 30.86 % in output torque and 29.34% in input torque for the HE-CMG compared to RPMG, attributed to the design trade-offs introduced by hybrid excitation. Additionally, Figure 9 also shows the presence of torque ripple in both input and output torque profiles for both gear models.

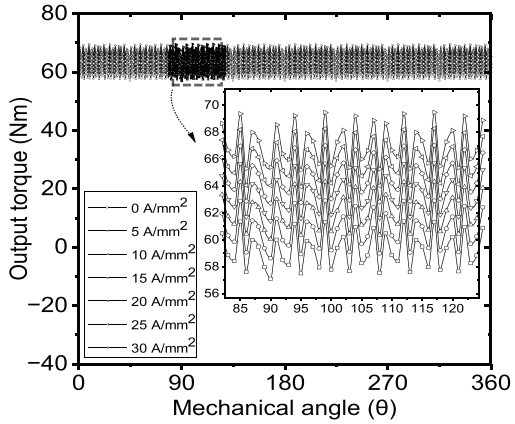

Fig. 7. Torque curve for the output rotor for the proposed HE-CMG under different current densities

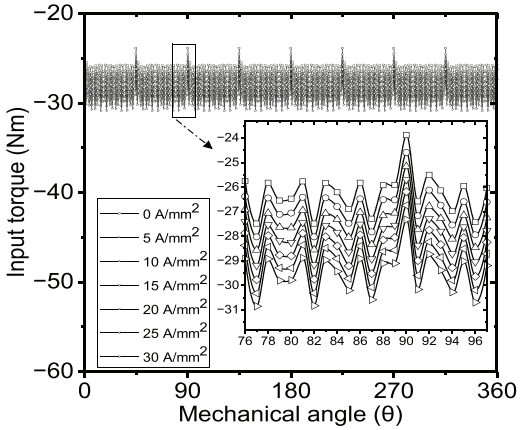

Fig. 8. Torque curve for the input rotor for the proposed HE-CMG under different current densities

Static Torque Evaluation

Static torque measurement is essential for determining the maximum load a magnetic gear can withstand before slippage or failure occurs. This parameter is a critical performance index for evaluating a CMG's load-handling capability and overall robustness, particularly under startup and heavy-load conditions. In static torque simulations, one rotor, typically the low-speed rotor connected to the load, is held stationary, while the high-speed rotor, attached to the prime mover, is rotated. This study evaluated static torque by fixing the FMP rotor and rotating the IPP rotor at a speed of 120 r/min.

Figure 10 presents the static torque profiles of the proposed HE-CMG and RPMG across one electrical cycle. The torque waveform exhibits a sinusoidal pattern, consistent with a transmission ratio of 2.4, and closely mirrors the characteristics observed in the RPMG. The variation in torque as a function of electrical angle follows a typical sine wave trend, with the peak torque occurring at an electrical angle of 90°, indicating the maximum static torque point of the system. This peak value provides critical information for validating the gear's rated torque transmission capability.

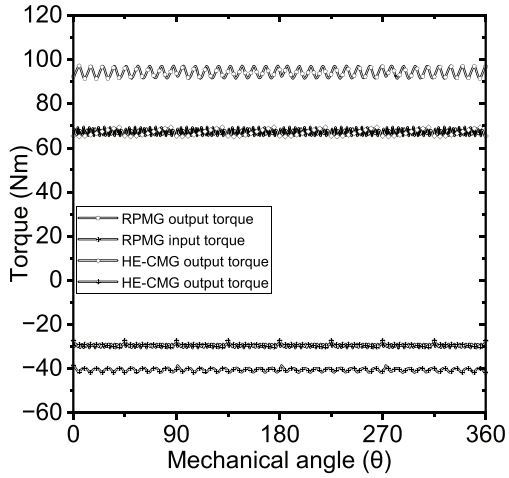

Fig. 9. Dynamic torque-mechanical angle waveforms

The input static torque (from the IPP rotor) for the RPMG and HE-CMG is 41.05 Nm and 30.97 Nm, respectively, corresponding to a reduction of 24.56 % in the HE-CMG. Similarly, the output static torque (from the FMP rotor) is 93.98 Nm for the RPMG and 67.22 Nm for the HE-CMG, reflecting a 28.47% decrease.

Torque Transmission Efficiency

Torque transmission efficiency is a critical metric for assessing the effectiveness of MG systems in con-

verting input into usable output torque. It is calculated based on the ratio of output to input mechanical power, P_o and $P_{i,}$ where mechanical power is the product of the torque and angular speed. Since the torque values are captured in transient mode, integral averaging ensures accuracy. The torque efficiency is defined as:

$$G_{Eff} = \frac{P_o}{P_i} \times 100\% = \frac{\tau_o \omega_o}{\tau_i \omega_i} \times 100\% \quad (8)$$

where τ_i and τ_o are the input and output torques, respectively, and ω_i and ω_o are the angular speeds of the input and output rotors, respectively.

The results reveal that the RPMG and the proposed HE-CMG models achieve high transmission efficiencies above 90 %, validating their practical utility in mechanical power transmission applications.

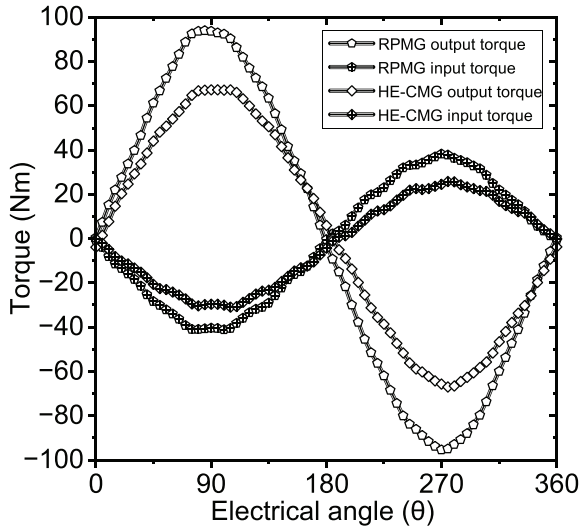

Fig. 10. Static torque-electrical angle waveforms

Torque Density

Torque density, $T_{D,}$ is a key parameter used to assess the compactness and torque capability of an MG. It is defined as the ratio between the maximum static electromagnetic torque at the output rotor and the total volume of the MG:

$$T_D = \frac{T_{MS}}{V_{MG}} \quad (9)$$

where T_{MS} is the maximum static electromagnetic torque and V_{MG} is the total volume of the gear.

The torque densities for the RPMG and HE-CMG are 144.36 kNm/m^3 and 103.26 kNm/m^3, respectively, indicating a performance trade-off in favour of reduced PM usage in the HE-CMG.

Torque to Excitation Material Mass Ratio

While torque density is widely used for evaluating MG performance, it includes structural components such as shafts, bearings, and yokes, potentially distorting the assessment of magnetic material efficiency [22]. A more precise indicator is the torque to PM ratio, T_{PM}, which also can be called as excitation torque density, T_{EM}, which isolates the torque contribution from the excitation source material alone:

$$T_{EM} = \frac{T_{MS}}{M_{EM}} \quad (10)$$

where M_{EM} is the total mass of the PMs or can be any other excitation material used. This metric provides a clearer view of the performance effectiveness per unit mass of magnetic material, aiding in material optimization efforts.

Overall Performance Comparison

Table 2 compares the electromagnetic and structural performance metrics of the RPMG and the proposed HE-CMG. The HE-CMG demonstrates notable material efficiency by reducing the PM mass from 1.05 kg in the RPMG to 0.758 kg, supplemented by only 0.125 kg of copper for excitation. Despite a 28.47 % reduction in output torque, the HE-CMG maintains a high excitation torque density (76.13 Nm/kg) with only a 14.94 % drop compared to the RPMG (89.5 Nm/kg). Moreover, both gear models achieve transmission efficiencies above 94 %, highlighting their suitability for practical applications. The HE-CMG's design showcases a balanced trade-off between torque performance and material efficiency, making it a strong candidate for future sustainable transmission systems.

Conclusion

The paper presents the design and two-dimensional finite element analysis (2D FEA) of a HE-CMG featuring DC-excited FECs wound within the closed stator slot. The design process was thoroughly detailed, including key parameters, geometrical dimensions, and material selections. Parametric simulations were conducted with excitation current densities up to 30 A/mm^2, identifying this value as optimal for maximizing torque transmission. When compared with RPMG, the HE-CMG exhibits a reduced output of 67.22 Nm versus 93.98 Nm. However, the excitation torque density only decreases marginally by 14.94 % (from 89.5 Nm/kg to 76.13 Nm/kg), demonstrating the effectiveness of hybrid excitation in maintaining high torque performance.

Table 2. Key design parameter comparison between RPMG and HE-CMG

Parameter	RPMG	HE-CMG
PM volume (m^3)	1.40×10^{-4}	1.01×10^{-4}
Copper volume (m^3)	-	1.40×10^{-5}
PM weight (kg)	1.05	0.758
Copper weight (kg)	-	0.125
MG volume (m^3)	6.51×10^{-4}	
Outer torque (Nm)	93.98	67.22
Torque density, T_D (kNm/m^3)	144.36	103.26
Excitation torque density, T_{EM} (Nm/kg)	89.50	76.13
Transmission efficiency (%)	96.60	94.54

Notably, the HE-CMG achieves this performance using significantly less PM material, 0.292 kg less, by supplementing with 0.125 kg of copper windings. This reduction indicates a more material-efficient design while maintaining acceptable performance levels. Overall, the HE-CMG offers a promising balance between torque density, excitation torque density, and material usage, suggesting strong potential for practical applications where cost, sustainability, and rare-earth material constraints are concerns. Future work may focus on enhancing performance through FEC slot geometry optimization, alternative winding configurations, and structural refinements. These improvements could further elevate the performance and functional competitiveness of the HE-CMG for advanced electric drive and magnetic gear applications.

Acknowledgments: *This research work is funded by the Malaysian Ministry of Higher Education (MoHE) through the Fundamental Research Grant Scheme (FRGS), No: FRGS/1/2024/TK08/UTEM/02/3. The authors would also like to thank Universiti Teknikal Malaysia Melaka (UTeM) for all the support.*

Received: 16.07.2025, **Accepted:** 08.09.2025, **Published:** 29.09.2025

REFERENCES

[1] Z. Su and L. Jing, "Multi-Objective Optimization Analysis of Auxiliary Flux Modulator Magnetic Gear with Unequal Magnetic Poles," in CES Transactions on Electrical Machines and Systems, vol. 7, no. 4, pp. 372-378, December 2023, doi: 10.30941/CESTEMS.2023.00040.

[2] Halim, M. (2024). Concentric Magnetic Gear Structure Review. PRZEGLĄD ELEKTROTECHNICZNY, 1(8), 142–149. https://doi.org/10.15199/48.2024.08.29.

[3] Y. Ghorbani, I. M. S. K. Ilankoon, N. Dushyantha, and G. T. Nwaila, "Rare earth permanent magnets for the green energy transition: Bottlenecks, current developments and cleaner production solutions," Resour Conserv Recycl, vol. 212, p. 107966, 2025, doi: https://doi.org/10.1016/j.resconrec.2024.107966.

[4] Z. Thelen et al., "Performance of Ideal and Practical Concentric Magnetic Gears in High Speed Applications," 2024 21st International Conference on Harmonics and Quality of Power (ICHQP), Chengdu, China, 2024, pp. 491-496, doi: 10.1109/ICHQP61174.2024.10768732.

[5] L. Jing, Z. Huang, J. Chen and R. Qu, "An Asymmetric Pole Coaxial Magnetic Gear With Unequal Halbach Arrays and Spoke Structure," in IEEE Transactions on Applied Superconductivity, vol. 30, no. 4, pp. 1-5, June 2020, Art no. 5200305, doi: 10.1109/TASC.2019.2962687.

[6] L. Jing, J. Gong, Z. Huang, T. Ben and Y. Huang, "A New Structure for the Magnetic Gear," in IEEE Access, vol. 7, pp. 75550-75555, 2019, doi: 10.1109/ACCESS.2019.2919679.

[7] L. Cao, K. T. Chau, C. H. T. Lee, W. Li and H. Fan, "Design and Analysis of Electromagnetic Gears With Variable Gear Ratios," in IEEE Transactions on Magnetics, vol. 53, no. 11, pp. 1-6, Nov. 2017, Art no. 8204706, doi: 10.1109/TMAG.2017.2716837.

[8] T. F. Megahed et al., "Innovative Magnetic Gear Design Incorporating Electromagnetic Coils for Multiple Gear Ratios," Machines, vol. 12, no. 10, Oct. 2024, doi: 10.3390/machines12100690.

[9] L. Jing, Z. Huang, J. Chen, and R. Qu, "Design, Analysis, and Realization of a Hybrid-Excited Magnetic Gear during Overload," IEEE Trans Ind Appl, vol. 56, no. 5, pp. 4812–4819, Sep. 2020, doi: 10.1109/TIA.2020.3004425.

[10] M. F. M. Ab Halim, A. Ab Rahman, M. S. Yahaya, and E. Sulaiman, "Hybrid-excited magnetic gear topology for improved gear efficiency at increasing rotor speed," International Journal of Power Electronics and Drive Systems, vol. 15, no. 1, pp. 91–97, Mar. 2024, doi: 10.11591/ijpeds.v15.i1.pp91-97.

[11] Gundogdu, T., & Komurgoz, G. (2013). The impact of the selection of permanent magnets on the design of permanent magnet machines - a case study: Permanent magnet synchronous machine design with high efficiency. Przeglad Elektrotechniczny, 89(3 A), 103-108.

[12] M. M. Firdaus A Halim, E. Sulaiman, R. N. F K R Othman, H. Onn Malaysia Parit Raja, and J. Malaysia, "Flux modulated rotating pole piece magnetic gear," International Journal of Power Electronics and Drive Systems (IJPEDS), vol. 11, no. 4, pp. 1731–1736, Dec. 2020, doi: 10.11591/IJPEDS.V11.I4.PP1731-1736.

[13] Yifei Yang, Zhi Hua Liang, and Chun Hua Sun, "Performance Analysis of Stator Hybrid Excitation Magnetic Planetary Gear Machines," Progress In Electromagnetics Research M, Vol. 92, 147-155, 2020. doi:10.2528/PIERM20022701

[14] M. Harke, "Fractional Slot Windings with a Coil Span of Two Slots and Less Content of Low Order Harmonics," 2018 International Symposium on Power Electronics, Electrical Drives, Automation and Motion (SPEEDAM), Amalfi, Italy, 2018, pp. 1309-1314, doi: 10.1109/SPEEDAM.2018.8445278.
[15] D. Danielczyk, "Analysis and experimental verification of dual star permanent magnet synchronous motor with rotor back iron made of soft magnetic composite," PRZEGLĄD ELEKTROTECHNICZNY, vol. 1, no. 7, pp. 14–19, Jul. 2019, doi: 10.15199/48.2019.07.03.
[16] Sato, M., Takazawa, K., Horiuchi, M., Masuda, R., Yoshida, R., Nirei, M., Bu, Y., & Mizuno, T. (2020). Reducing Rotor Temperature Rise in Concentrated Winding Motor by Using Magnetic Powder Mixed Resin Ring. Energies, 13(24), 6721. https://doi.org/10.3390/en13246721.
[17] Frosini, L., & Pastura, M. (2020). Analysis and Design of Innovative Magnetic Wedges for High Efficiency Permanent Magnet Synchronous Machines. Energies, 13(1), 255. https://doi.org/10.3390/en13010255.
[18] S. Pirzad, A. A. Ghadimi, A. H. Abolmasoumi, A. Jabbari, and S. Bagheri, "Optimal mixed control of Axial Flux Permanent Magnet Synchronous generator wind turbines with modular stator structure," ISA Trans, vol. 115, pp. 153–162, 2021, doi: https://doi.org/10.1016/j.isatra.2021.01.001.
[19] R. Tsunata, M. Takemoto, J. Imai, T. Saito and T. Ueno, "Comparison of Thermal Characteristics in Various Aspect Ratios for Radial-Flux and Axial-Flux Permanent Magnet Machines," in IEEE Transactions on Industry Applications, vol. 59, no. 3, pp. 3353-3367, May-June 2023, doi: 10.1109/TIA.2023.3255845.
[20] M. Zheng, Z. Q. Zhu, S. Cai and S. S. Xue, "A Novel Modular Stator Hybrid-Excited Doubly Salient Synchronous Machine With Stator Slot Permanent Magnets," in IEEE Transactions on Magnetics, vol. 55, no. 7, pp. 1-9, July 2019, Art no. 8104409, doi: 10.1109/TMAG.2019.2902364.
[21] L. Jing, J. Gong, J. Chen, Z. Huang and R. Qu, "A Novel Coaxial Magnetic Gear With Unequal Halbach Arrays and Non-Uniform Air Gap," in IEEE Transactions on Applied Superconductivity, vol. 30, no. 4, pp. 1-5, June 2020, Art no. 5000105, doi: 10.1109/TASC.2020.2968043.
[22] V. Mateev, I. Marinova and M. Todorova, "Torque and Power Density of Coaxial Magnetic Gears," 2019 II International Conference on High Technology for Sustainable Development (HiTech), Sofia, Bulgaria, 2019, pp. 1-5, doi: 10.1109/HiTech48507.2019.9128272.